REGULAR ARTICLE

Novel Nanopigments with a Thiazole Moiety for Printing Paper, Carton, and Polyester Fabrics: Synthesis, Characterization, and Color Strength with Comparative Study

Hala F. Rizk[1] · Mohamed A. El-Borai[1] · Osama M. Hemeda[1] · Seham A. Ebrahim[1] · Mohamed E. Sadek[1]

Abstract

A series of new coloring materials in nanoscale based on 5-(2-aminothiazol-5-yl) thiazol-2-amine and 5-(4-aminophenyl) thiazol-2-amine were synthesized. The nanoscale pigments were prepared using a grinding high-energy ball-milling technique. X-ray diffraction and transmission electron microscopy were employed to determine the particle size of the nanoscale pigments (40–80 nm). The synthesized pigments in normal and nanoscale were applied in the printing of polyester fabrics. The fastness and colorimetric properties of the printed samples were carefully studied. Additionally, the synthesized pigments were applied as water-based flexographic ink for paper and carton. The hue of the color pigments L^*, a^*, b^*, glossiness, and fastness to light were measured. The comparison of the new heterocyclic benzidine analogs in normal and nanoscale with commercial benzidine pigments demonstrated better results, particularly for the nanoscale pigments.

Keywords 2-Amino thiazole · Diarylide pigments · Nanopigments · Ball-milling technique · Water-based flexographic ink
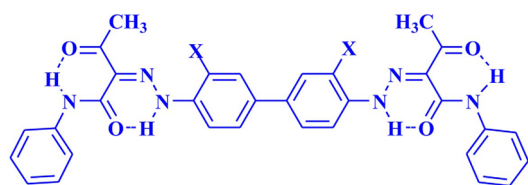
1 Introduction

Printing with pigments is the oldest and easiest printing method for its simple application [1–5]. Most good printed textiles, paints, inks, plastics, and rubbers have been printed with pigment dyestuff because they provide strong and bright hues with a complete color spectrum. In addition, they exhibit good weather and acid/alkali resistance [6–12]. These pigments offer advantages over dyes because of their short dyeing time, low chemical usage, less effluence, and nonfiber selectivity [13]. Painting dispersing systems depend on the medium used (solvent- and water-based pigments).

✉ Hala F. Rizk
 dr_hala_fawzy@yahoo.com

1 Department of Chemistry, Faculty of Science, Tanta University, Tanta 31527, Egypt

Water-based pigment systems are eco-friendly pathways because of the presence of auxiliaries (dispersants, emulsifiers, and antisetting agents). This technique has been widely applied in dyeing textiles, paints, architecture, and wood [14, 15]. The major problem of pigments is their poor dispersing stability due to the particle size and surface charge, owing to the imperfection of the dispersants [16]. As the particle size of pigments increases, the painting suffers from problems because the precipitation, floating color, color fastness, ease of handling, and uniformity of the fabrics dyed with the unmodified pigment dispersion are influenced. However, it is difficult to obtain pigment particles that are smaller than 100 nm. By modifying the pigment surface, the average diameter of pigment particles can be reduced to a range of 100–200 nm. Nanometer- or micrometer-sized pigment, so called ultrafine modified pigment (UMP), can be obtained by physical modification through the mechanical action provided by high impact mill equipment, such as the sand and ball mill and/or chemical modification in a composite dispersion system, attaching functional groups for pigment dispersion to provide pigment dispersion with high stability and color strength approaching that of dyestuffs [17]. Using the water-based nanopigment technique, the UMP particles aggregate and agglomerate. Therefore, we used ultrasonic energy as an environmental and efficient approach [18],
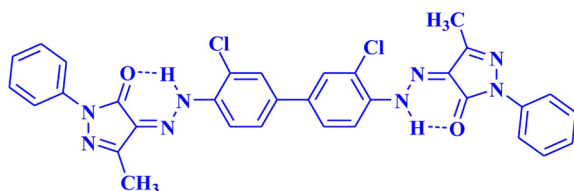
PG1   X = –Cl
PG2   X = –OCH₃

PG3

Fig. 1 Structure of commercial pigments (PG1–PG3)

PG4   Ar = –C₆H₆
PG5   Ar = 4-CH₃-C₆H₅

Fig. 2 Structure of synthesized pigments (PG4–PG5)

PG6   Ar = –C₆H₆
PG7   Ar = 4-CH₃-C₆H₅

Fig. 3 Structure of synthesized pigments (PG6–PG7)

PG8 Ar = C₆H₆
PG9 Ar = 4-CH₃-C₆H₅

Fig. 4 Structure of synthesized pigments (PG8–PG9)
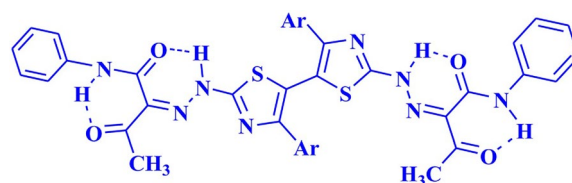

PG10 Ar = -C₆H₆
PG11 Ar = 4-CH₃-C₆H₅

Fig. 5 Structure of synthesized pigments (PG10–PG11)

mainly because of the phenomenon known as cavitation in a liquid medium [19]. The pretreatment of pigments by ultra-sonication has been widely applied in dyeing and finishing processes in the painting of textiles.

Diarylide pigments are a class of colored organic diazo compounds prepared from substituted benzidine and aceto-acetanilide or pyrazolone or their derivatives [20]. They are coloring agents that are primarily used in ink and toners to create images. They are also used in paints and coatings, food packaging, plastics, and rubber materials [21–23]. They are frequently yellow or orange. Owing to their brilliant hues and high tinting strength, diarylide yellow pigments are popular among ink manufacturers. They exhibit good printing capabilities and are cost-effective in terms of tinting strength per unit.
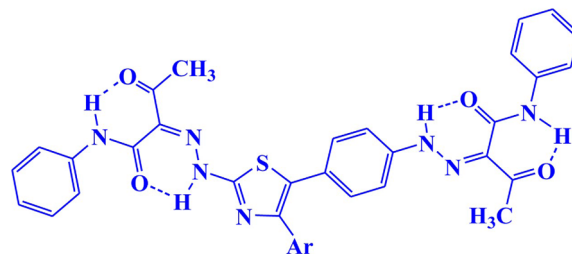
The commercial azobenzidine pigments synthesized from 3,3'-dichlorobenzidine and 3,3'-dimethoxybenzidine (Fig. 1) can be metabolized to benzidine, which is considered to be carcinogenic and classified as "reasonably anticipated to be human carcinogens" [24–27]. Our previous paper [28] discussed the synthesis, cytotoxicity, and antioxidant and anti-microbial activities of new heterocyclic pigments containing thiazole moiety alternatives for benzidine-based pigments (Figs. 2, 3, 4, 5). The newly synthesized pigments showed characters in good color and less toxicity.

This study physically synthesized nanoheterocyclic pig-ments using a ball-milling technique for a comparative study between the properties of new heterocyclic pigments in nor-mal and/or nanoscale and commercial benzidine pigments. Additionally, their applications in printing on paper, carton, and polyester fabrics were evaluated. The application of the new nanopigments via the pigment printing technique offers excellent color fastness and good ecological performance.
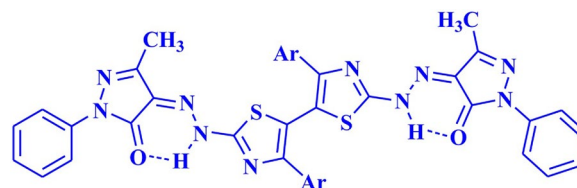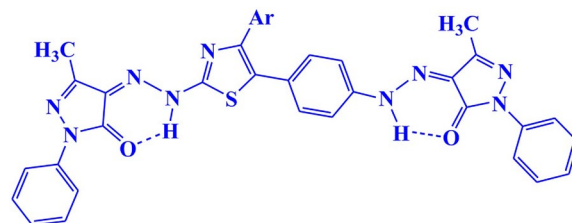
2 Experimental

2.1 Synthesis of New Pigments (PG4–PG11)

A new series of pigments based on 5-(2-aminothiazol-5-yl) thiazol-2-amine and 5-(4-aminophenyl)thiazol-2-amine were prepared as heterocyclic alternatives for benzidine-based mono and disazo dyestuffs (28).

2.2 Synthesis of Nanoscale Pigments (nPG1–nPG11)

nPG1–nPG11 were prepared by ball milling (VQ-N High Energy Ball Mill, Across International, USA). **PG1–PG11** were charged and dry mixed into 80 ml of stainless steel agar with eight grinding balls at 1200 rpm for 40 min. The prepared and commercial pigments, **nPG1**, **nPG3**, and **nPG4–nPG8**, were analyzed using a JEM-2100 high-resolution transmission electron microscope (JEOL-100SX, Japan).

2.3 Ultraviolet (UV)–Visible Spectral Determination

The absorption spectra of the new pigments in normal scale in different solvents and the nanopigments in dimethylformamide (DMF) were recorded using a Shimadzu (UV-310 PG) spectrophotometer using a 1.0-cm quartz cell.

2.4 General Procedure for the Printing of Polyester Fabrics

The print paste was prepared by stirring 5.8 g of sodium alginate (thickener) in 19 ml of hot H_2O, 3.25 g of different pigments, 15.5 g of polyurethane acrylate (PUA) (binder), and 10 ml of polyethylene glycol. The print paste was gradually added to a homogeneous thickener suspension. After complete addition, the nanopigment mixture was exposed to ultrasonic radiation to prevent the coagulation of nanoparticles.

A 70-mesh flat printing screen and 10-mm diameter squeegee were used for the printing process, at a printing speed of 4 m/min and pressure grade of 1. The printing was performed on a Johannes Zimmer-type MDK laboratory machine. A Mathis laboratory dryer machine was used to dry and cure the printed samples at 100 °C for 10 min. Fabrics with rectangular prints were used (10×30 cm). Standard test methods were employed to evaluate the printed fabrics.

2.5 General Procedure for the Printing of Paper and Carton

Here, 16 g of pigment was gradually added to 40 g of acrylic resin (Joncryl 678 from BASF Company), 5 g of a dispersing agent, 8 g of monoethanolamine (paste should be within a pH of 8–9), 1 g of deformer, and 130 g of water. The mixture was stirred for 20 min using a high-speed stirrer at 1000 rpm. Thereafter, 200 g of glass beads was added to the paste of the color solution in a 500-m*l* jar, and the mixture was ground for 90 min at 100 rpm in a laboratory grinding machine until the particles were 5 µm. The paste was filtered after grinding and a drop was taken in an RK Lab machine for printing on white paper.

2.6 Measurement of Printing Properties

2.6.1 Fastness to Light

The specimen of the printed textile was exposed to light from a xenon arc in a well-ventilated exposure chamber, following dyed wool standards. The chamber was maintained at a constant temperature of 30 °C. The humidity was maintained at $45 \pm 5\%$ effective humidity. The difference in light between the intensity of the specimen and the standards should not exceed 20%. The samples and standards were exposed for the same amount of time under the same conditions. The samples were viewed in the light from a day-light fluorescent lamp and assigned a degree in comparison with the relative to blue scale (1–8) standards of the American Association of Textile Chemists and Colorists (Tables 3 and 5).

2.6.2 Colorimetric Analysis

The colorimetric parameters of the dyed polyester fabrics were measured using a reflectance spectrophotometer (Gretag-Macbeth CE-7000A). The system was equipped with a D65/10° source and barium sulfate as a standard blank and three repeated measurement average settings. The assessment of color-dyed fabrics was performed using a tristimulus colorimeter [29].

3 Results and Discussion

3.1 Characterization of nPG1, nPG3, and nPG4–nPG8

The synthesis of nanopigments by high-energy ball milling afforded a suitable particle size. This was performed for a particle size range of 8–20 nm. The size was estimated using X-ray diffraction (XRD) (Fig. 6).
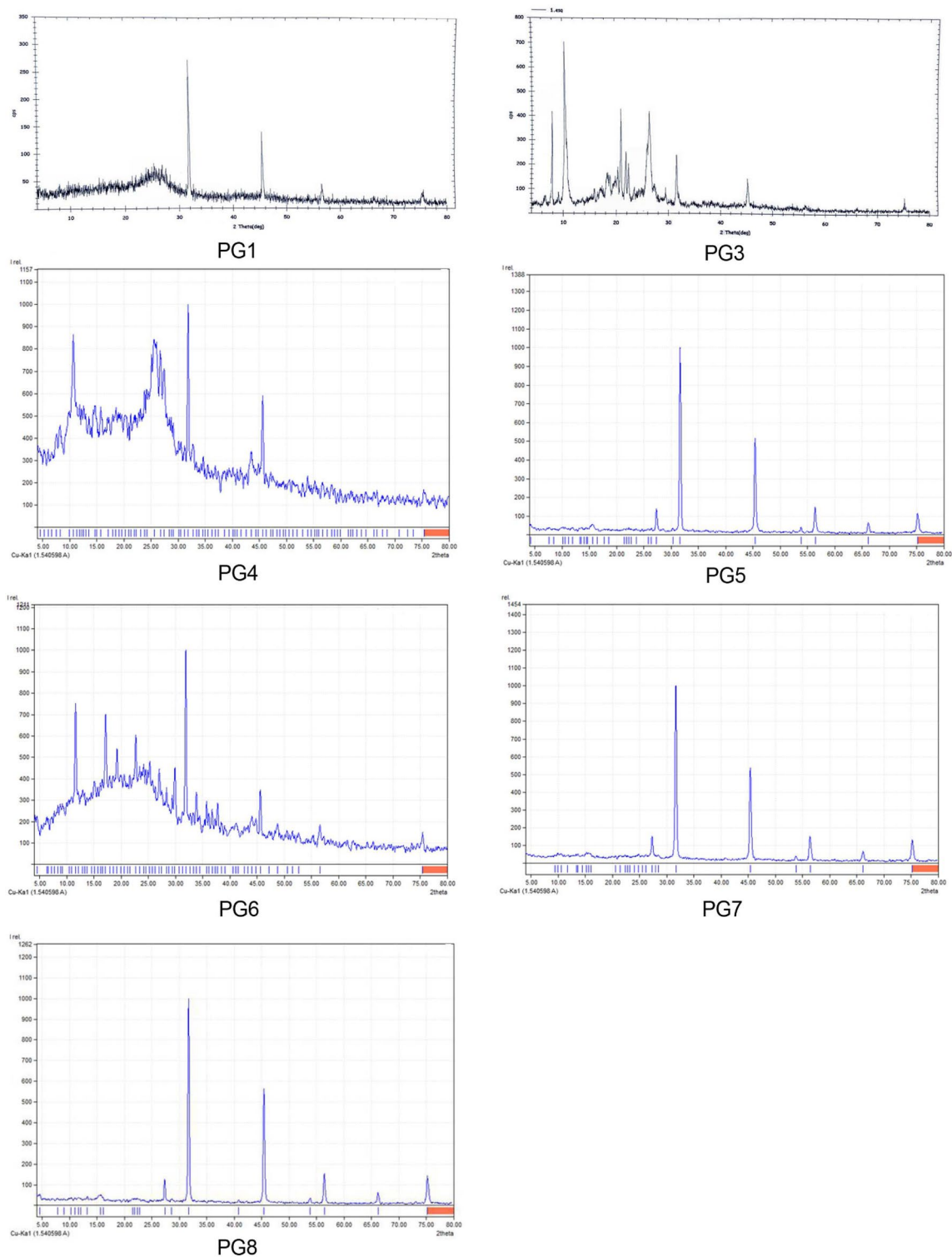
Fig. 6 XRD patterns for certain commercial and synthesized pigments

All materials scatter X-rays, but only ordered or crystalline components afford distinct fingerprint diffraction patterns. The other phases were less intense. Each major phase was identified by the presence of the most intense line measuring more than several times the local noise level in the diffraction pattern and the presence of supplementary lines. Berrie identified dolomite, quartz, gypsum, calcite, and ferrous compounds in comparable Tiepolo ground layer

samples findings, which correlated with the present results [30]. Therefore, only crystalline pigments and additives can be identified by XRD. Consequently, the degree of background noise observed in a spectrum indicates the relative amorphous content; the higher the ratio of background to the peak height, the greater is the amorphous content, as shown in PG2, PG3, and PG4. The crystalline nature of the product was revealed by the extremely sharp and intense peaks in the XRD patterns. The homogeneous and crystalline nature of PG3, PG5, PG7, and PG8 was observed. The other samples exhibited mixed crystalline and amorphous phases.

The absence of other diffraction lines in the scanned region suggested the use of organic or noncrystalline pigments and demonstrated the limitation of the technique in its ability to identify many modern pigments that are often amorphous organic species. However, it is valuable for identifying filler or bulking agents, which are minerals, such as calcite magnesium silicate (talc) or kaolin and the ubiquitous modern white titanium dioxide.

The average crystallite size (D) is calculated using the Scherrer's equation as follows:

$$D = 0.9\lambda/(h_{1/2}cos\theta_B),$$

where λ is the wavelength for Cu-Kα (λ = 1.5405 Å), $h_{1/2}$ is the full width at half maximum of the diffraction peak (in radian), and θ_B is the diffraction angle.

The transmission electron microscopy (TEM) images of the nanopigments are shown in Fig. 7. It was observed that the nanopigments comprised particles with distribution within 9–15 nm. XRD is useful for determining crystal size but does not provide information on the size distribution, whereas TEM can be employed to provide information on the shape and size distribution of the nanoparticles. The HRTEM image for **PG3** shows lattice spacing, confirming the crystalline nature of the sample. The interplanar distance is correlated with the XRD results. The micrograph shows rod-like particles in an agglomerated state [31]. The same result was obtained from the analysis of the XRD pattern using Scherrer's equation. The crystallite size obtained from XRD and the particle size from TEM are listed in Table 1.

High value of the crystallite size obtained by TEM due to the agglomeration of the pigment particles, which had high adhesive force.

Agglomeration was observed in the images, which essentially reflected the ability of the pigment to stick to fabrics.

3.2 UV–Visible Spectral Analysis

The electronic absorption spectra of the synthesized pigments, PG4–PG11, were recorded in three solvents representing three categories of organic solvents: acetonitrile (polar aprotic solvent), DMF, and dimethyl sulfoxide

(DMSO) (dipolar aprotic solvent). The visible maximum absorption for the synthesized pigments was measured and is listed in Table 2 and Figs. 8, 9, 10.
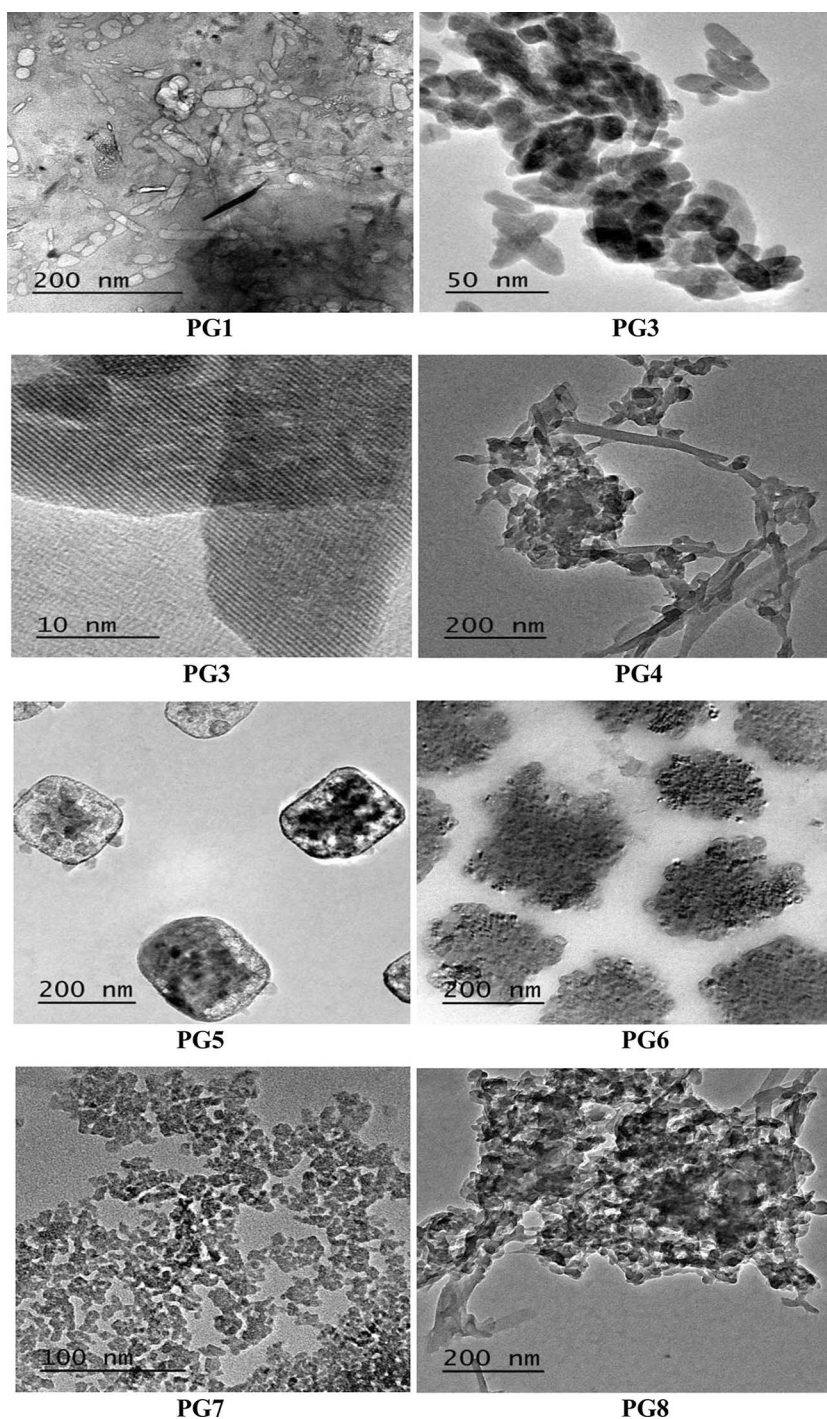
3.2.1 UV–Visible Absorption Spectra of Pigments in Normal Scale

Most pigments are practically insoluble in common organic solvents, but the introduction of bulky groups in the 4,4′-positions of the bithiazolyl linkage increased the solvent solubility of the pigments, thereby allowing UV–visible measurements to be conducted in solution. The differences in the λ_{max} values in solution versus the solid state may have been due to conformational changes upon shifting from the solution to the solid phase, changes involving intramolecular H-bonding and/or intermolecular p–p interactions, and light scattering from the pigment particles. The molecules existed in the bis-keto-hydrazone tautomeric form. The intramolecular hydrogen bonding normally associated with this structural arrangement was observed, but intermolecular hydrogen bonding was not observed. Our attempts to fully understand the influence of the nature of the solvent on the spectra of the series of diazo pigments were limited by the extreme insolubility of the materials in a wide range of solvents. However, the compounds exhibited reasonable solubility in DMF, DMSO, and CH$_3$CN. The spectral data in these solvents are listed in Table 2. The single visible absorption band in the spectra of the diazo pigments in each case indicated a large bathochromic shift in DMF, compared with DMSO and CH$_3$CN. These results supported the hypothesis that diazo chemicals only existed in the ketohydrazone form. The prepared pigments exhibited a considerably higher molar absorptivity, ε (extinction coefficient). Notably, among the series of investigated pigments, the previously unreported disazo pigment exhibited the highest color strength per unit weight.

3.2.2 UV–Visible Absorption Spectra of Nanopigments

UV–visible absorption spectra were recorded for the dried nanopigments dispersed in DMF and corresponding pigments dissolved in DMF as a reference solvent. Compared with the maximum absorption wavelength (λ_{max}) of the corresponding dye, the λ_{max} of each nanopigment exhibited a slight bathochromic shift (Fig. 11) i.e., 424 vs. 420 nm of PG4, 409 vs. 404 nm of PG5, 384 vs. 379 nm of PG7, 420 vs. 395 nm of PG8, 422 vs. 417 nm of PG9, 429 vs. 420 nm of PG10, and 428 vs. 418 nm of PG11. This was because the nanopigment had a highly extended π-conjugated planar structure, which generated intermolecular π–π* interaction and led to molecular stacking. Therefore, we concluded that the separated dye phase embedded in the polymeric matrix
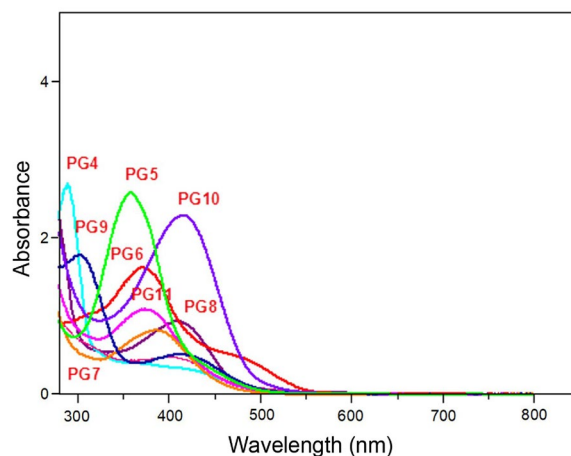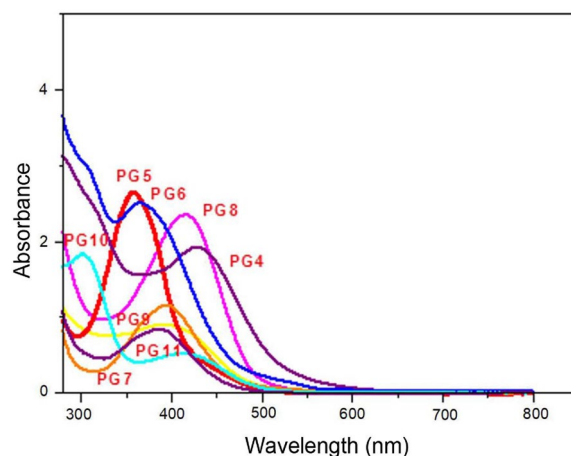
["

Table 1 Crystallite size from XRD and particle size from TEM with x content

Pigment no.	Crystallite size (nm) from XRD	Crystallite size (nm) from TEM
PG1	17.3	20
PG3	20.2	22.1
PG4	15.04	16
PG5	9.29	11.1
PG6	8.79	10.5
PG7	8.26	9.6
PG8	9.22	11.1

Fig. 8 Absorption spectra of PG4–PG11 in acetonitrile (1×10^{-5} M)

coordinates indicated that the color hues of the pigments under investigation shifted to the yellowish direction on the yellow–blue axis according to the positive values of b^* and the reddish direction on the red–green axis, according to the positive values of a^*. Conversely, the new pigment, **PG4**, for normal particles, yielded higher K/S values, compared with the benzidine commercial pigments, indicating that the color strength on polyester fabrics increased. In addition, most particles in normal scale are brighter than those in nanoscale. **PG4** and **PG5** in normal scale were brighter, compared with the other synthesized benzidines, and were similar to the commercial pigment, **PG2**.

3.4 Water-based Flexographic Ink and Color Assessments of the Synthesized Pigment and Commercial Benzidine Pigments on Paper and Carton

The synthesized pigments were applied as water-based flexographic ink for printing paper and carton. The results obtained are shown in Table 4. The pigments derived from benzidene, **PG1, PG2,** and **PG3** and/or the pigment derived from the coupling of diazonium thiazole salt with pyrazolone exhibited difficult compatibility but more color

Fig. 9 Absorption spectra of PG4–PG11 in DMSO (1×10^{-5} M)

strength. Furthermore, **PG2, PG5,** and **PG6** exhibited an extremely good shade of pure yellow and were glossy. **PG8, PG9, PG10,** and **PG11** exhibited a reddish shade

Table 2 Absorption data of synthesized pigments (PG4–PG11)

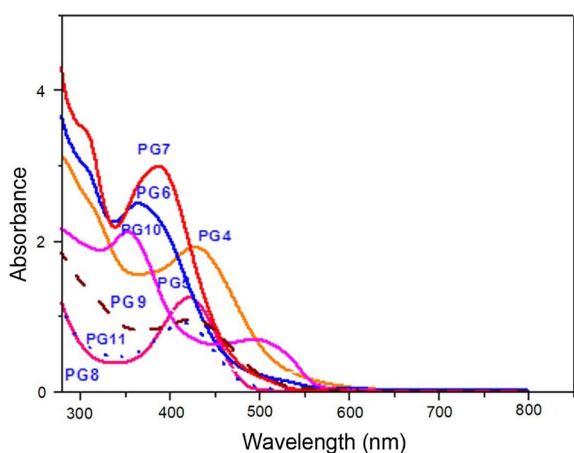| Pigment no.	Absorption λ_{max}(nm) (DMF)	$\varepsilon_{max} \times 10^4$ (lmol^{-1} cm^{-1})	Absorption λ_{max}(nm) (DMSO)	$\varepsilon_{max} \times 10^4$ (lmol^{-1} cm^{-1})	Absorption λ_{max} (nm) (Acetonitrile)	$\varepsilon_{max} \times 10^4$ (lmol^{-1} cm^{-1})
PG4	427	9.40	427	9.65	372	2.80
PG5	400	2.00	357	3.30	357	6.50
PG6	366	2.49	366	12.20	372	4.10
PG7	387	12.90	393	5.74	385	4.18
PG8	425	6.20	417	5.57	359	6.50
PG9	500	1.945	400	2.30	393	1.30
PG10	396	10.30	415	1.30	419	1.30
PG11	415	4.515	385	4.18	377	1.30

Fig. 10 Absorption spectra of PG4–PG11 in DMF (1×10^{-5} M)

Fig. 11 Absorption spectra of PG4–PG11 and their nanopigments in DMF (1×10^{-5} M)

Table 3 Color assessments and light fastness of the synthesized pigments in normal and nanoscale and commercial benzidine pigments on polyester fabrics

Light Fastness	K/S	R%	b	a	L	Color	No.
5	4.4	9.3	21.2	5.2	75.31		**PG1**
4	10.9	4.2	32.4	14.2	60.33		**PG1n**
5	16.8	2.8	52.5	11.6	58.64		**PG2**
4	11.5	4	42.1	8.5	68.62		**PG2n**
4	17.5	2.7	55.76	17.95	59.45		**PG3**
4	3.16	12.2	18.3	1.1	80.26		**PG3n**
6	19.8	2.4	49.4	20.3	57.31		**PG4**
3	3.8	10.5	19.8	1.9	78.51		**PG4n**
5	6.2	6.9	54.8	1.4	58.28		**PG5**
2	2.28	15.6	11,5	1.4	85.64		**PG5n**
2	3.9	10.2	22.5	3.5	69.66		**PG6**
2	3.3	11.6	16.6	2.6	70.36		**PG6n**
3	4.3	9.5	16.5	2.2	78.93		**PG7**
2	2.89	13.1	6.2	1.1	86.60		**PG7n**
5	4.05	9.98	51.4	10.5	63.41		**PG8**
5	10.2	4.52	41.44	13.3	62.79		**PG8n**
3	3.4	11.5	18.7	1.7	79.32		**PG9**
4	11.3	4.2	40.1	9.2	66.53		**PG9n**
3	9.65	4.7	31.3	12.3	68.35		**PG10**
4	10.38	4.4	40.4	9.5	62.14		**PG10n**
2	4.48	9.2	15.4	2.3	82.61		**PG11**
4	5.7	7.4	26.4	11.3	75.44		**PG11n**

exhibited medium-strength color, and could be used in water-based ink.

The CIELAB coordinates of the prepared pigments indicated that their color hues on paper and carton shifted to the yellowish direction on the yellow–blue axis, according to the positive values of b^* and shifted to the reddish direction on the red–green axis, according to the positive values of a^* except for **PG1** and **PG7**, which shifted to the greenish direction on the red–green axis, according to the negative values of a^*. The benzidine pigment, **PG3**, shifted to the blueish direction on the yellow–blue axis, according to the negative values of b^* and shifted to the greenish direction on the red–green axis, according to the negative values of a^*. Additionally, the light fastness on printed paper and carton was excellent (**7**) for the synthesized pigments. The results are grouped in Table 5.

4 Conclusion

Here, heterocyclic benzidine analogs with a thiazole moiety and commercial benzidine pigments were synthesized in nanoscale by grinding with a high-energy ball-milling technique. XRD and TEM were employed to determine

of yellow, good compatibility, and can be used in printing ink for paper and carton. **PG7** was the best because it exhibited an extremely good shade of pure yellow and was glossy. Generally, all the pigments were good, compatible,

Table 4 Performances of the synthesized pigments and commercial benzidine pigments (PG1–PG11) on paper and carton

Pigment no.	Compatibility in water-based ink	Shade	Notes
PG1	Good	Clear lemon	Can be used in printing ink for paper and carton
PG2	Very good	Reddish yellow	Can be used in water-based printing ink
PG3	Good	Brownish yellow	Hard to use in water-based printing ink because of high viscosity and tacky behavior
PG4	Very good	Greenish yellow	Can be used in printing ink for paper and carton
PG5	Very good	Reddish yellow	Can be used in printing ink for paper and carton
PG6	Very good	Reddish yellow	Can be used in printing ink for paper and carton
PG7	Very good	Faint glossy yellow	Very good use in water-based printing ink
PG8	Good	Brownish yellow	Can be used in printing ink for paper and carton
PG9	Good	Faint brownish yellow	Can be used in printing ink for paper and carton
PG10	Good	Bright yellow	Can be used in printing ink for paper and carton
PG11	Good	Reddish yellow	Can be used in printing ink for paper and carton

Table 5 Color assessments and light fastness of the synthesized and commercial pigments on paper and carton

Pigment no	L^*	a^*	b^*	Light fastness
PG1	−0.02	-5.68	−40.37	7
PG2	79.53	10.91	37.98	7
PG3	−19.07	17.62	0.80	7
PG4	82.93	0.32	53.87	7
PG5	77.52	12.72	40.36	7
PG6	8.62	17.01	41.19	7
PG7	88.33	-7.26	41.65	7
PG8	84.82	4.01	18.95	7
PG9	86.65	0.14	30.23	7
PG10	89.2	−6.17	37.29	7
PG11	85.71	−0.3	40.99	7

the particle size of the nanopigments. The synthesized pigments in normal and nanoscale and the benzidine pigments were applied for the printing of polyester fabrics and as water-based flexographic ink for paper and carton. The fastness and colorimetric properties were measured and compared with those of the benzidine pigments. The results showed that **PG4** and **PG5**, which were synthesized from the coupling of diazonium thiazole salt with aceto-acetanilide derivatives afforded a light hue and the best light fastness for the printing on polyester fabrics. **PG7** exhibited an extremely good shade of pure yellow and was glossy on paper and carton. This study followed the progress of the synthesis, toxicity, and characterization of other heterocyclic alternatives for benzidine-based pigments to achieve pigments with high fastness properties, attractive color, and eco-friendly behavior.

Data availability The datasets generated and analysed during the current study are available from the corresponding author on reasonable request.

Declarations

Conflict of interest The authors declare that they have no known competing financial interests or personal relationships that could have appeared to influence the work reported in this paper.

References

1. W. Schwindt, G. Faulhaber, Color. Technol **14**, 166 (1984)
2. M.M. El-Molla, Indian J. Fibre Text. Res. **32**, 105 (2007)
3. M.T. Islam, M.S. Farhan, F. Faiza, A.F.M. Fahad Halim, A.A. Sharmin, Colorants **14**, 38 (2022)
4. W. Schwindt, Melli. Textilberichte **71**, 693 (1990)
5. I. Holme, Color. Technol **22**, 1 (1992)
6. R. Assefi Pour, J. He, Coatings **10**, 78 (2020)
7. S.M. Burkinshaw, N. Kumar, Dyes Pigm. **80**, 53 (2009)

8. D. Fakin, A. Ojstrsek, S.C. Benkovic, J. Mater. Process Technol. **209**, 584 (2009)
9. Y. Zhang, W. Hou, Y. Tan, Dyes Pigm. **34**, 25 (1997)
10. H.Y. Wang, G.W. Wang, C.L. Zheng, T.J. Zhou, J. Sun, J. Appl. Polym. Sci. **135**, 9 (2018)
11. Z. Cai, Y. Qiu, J. Appl. Polym. Sci. **109**, 1257 (2008)
12. M.S. Abdelrahman, S.H. Nassar, H. Mashaly, S. Mahmoud, D. Maamoun, Coatings **10**, 58 (2020)
13. C.W. Kan, W.S. Man, Coatings **7**, 104 (2017)
14. Y. Kobayashi, H. Chiba, K. Mizusawa, N. Suzuki, J.M. Cerdá-Reverter, A. Takahashi, Gen. Comp. Endocrinol. **173**, 438 (2011)
15. Y. Lan, J. Lin, Dyes Pigm. **90**, 21 (2011)
16. K. Hayashi, H. Morii, K. Iwasaki, S. Horie, N. Horiishi, K. Ichimura, J. Mater. Chem. **17**, 527 (2007)
17. A.D. Bermel, D.E. Bugner, J. Imaging Sci. Technol. **43**, 320 (1999)
18. S.F. De Vallejuelo, A. Barrena, G. Arana, A. de Diego, J.M. Madariaga, Talanta **80**, 434 (2009)
19. X. Jia, C. Caroli, B. Velicky, Phys. Rev. Lett. **82**, 1863 (1999)
20. M. Nakpathom, D. Hinks, H. Freeman, Dyes Pigm. **48**, 93 (2001)
21. R.W. Dapson, Biotech. Histochem. **84**, 95 (2009)
22. M.A. Kamboh, I.B. Solangi, S.T. Sherazi, S. Memon, J. Hazard. Mater. **172**, 234 (2009)
23. S. Myintm, M.S. Zakaria, Kh.R. Ahmed, Prog. Rubber Plast. Recycl. Technol. **26**, 21 (2010)
24. T.M. Reid, K.C. Morton, C.Y. Wang, C.M. King, Environ. Mutagen. **6**, 705 (1984)
25. C.E. Cerniglia, J.P. Freeman, W. Franklin, L.D. Pack, Biochem. Biophys. Res. Commun. **107**, 1224 (1982)
26. C.E. Cerniglia, Z. Zhuo, B.W. Manning, T.W. Federle, R.H. Heflich, Mutat. Res. **175**, 11 (1986)
27. C.N. Martin, J.C. Kennelly, Carcinogenesis **2**, 307 (1981)
28. H.F. Rizk, M.A. El-Borai, A. Ragab, S.A. Ibrahim, M.E. Sadek, Polycycl. Aromat. Compd. (2021). https://doi.org/10.1080/10406638.2021.2015402
29. F.W. Billmeyer, M. Saltzman, *Principles of Color Technology*, 2nd edn. (Wiley-Interscience, New York, 1981)
30. C.L. Berrie, M.A. Langell, Surf. Interface Anal. **21**, 245 (1994)
31. J.R. Fryer, J. Microsc. **120**, 1 (1980)